Published in final edited form as:
Cell Res. 2012 February ; 22(2): 399–412. doi:10.1038/cr.2011.145.

K-ras^{G12V} transformation leads to mitochondrial dysfunction and a metabolic switch from oxidative phosphorylation to glycolysis

Yumin Hu[1,2,*], **Weiqin Lu**[2,*], **Gang Chen**[2,*], **Peng Wang**[1], **Zhao Chen**[2], **Yan Zhou**[2], **Marcia Ogasawara**[2], **Dunyaporn Trachootham**[2,3], **Li Feng**[2], **Helene Pelicano**[2], **Paul J Chiao**[4], **Michael J Keating**[5], **Guillermo Garcia-Manero**[5], and **Peng Huang**[1,2]

[1]State Key Laboratory of Oncology in Southern China, Sun Yat-Sen University Cancer Center, Guangzhou 510275, China [2]Department of Molecular Pathology, Unit 951, The University of Texas MD Anderson Cancer Center, 1515 Holcombe Boulevard, Houston, TX 77030, USA [3]Faculty of Dentistry, Thammasat University, Pathum-thani 12121, Thailand [4]Department of Surgical Oncology, The University of Texas MD Anderson Cancer Center, Houston, TX 77030, USA [5]Department of Leukemia, The University of Texas MD Anderson Cancer Center, Houston, TX 77030, USA

Abstract

Increased aerobic glycolysis and oxidative stress are important features of cancer cell metabolism, but the underlying biochemical and molecular mechanisms remain elusive. Using a tetracycline inducible model, we show that activation of K-ras^{G12V} causes mitochondrial dysfunction, leading to decreased respiration, elevated glycolysis, and increased generation of reactive oxygen species. The K-RAS protein is associated with mitochondria, and induces a rapid suppression of respiratory chain complex-I and a decrease in mitochondrial transmembrane potential by affecting the cyclosporin-sensitive permeability transition pore. Furthermore, pre-induction of K-ras^{G12V} expression *in vitro* to allow metabolic adaptation to high glycolytic metabolism enhances the ability of the transformed cells to form tumor *in vivo*. Our study suggests that induction of mitochondrial dysfunction is an important mechanism by which K-ras^{G12V} causes metabolic changes and ROS stress in cancer cells, and promotes tumor development.

Keywords

K-ras; mitochondrial dysfunction; glycolysis

Introduction

The difference between cancer cells and normal cells in their energy metabolism and redox states is an important research area that has gained increasing attention in recent years. Oxidative phosphorylation in the mitochondria and glycolysis in the cytosol are two major metabolic pathways that generate ATP in mammalian cells. Under physiological conditions, most normal cells use the more energy-efficient oxidative phosphorylation as the main route to generate ATP. In contrast, many cancer cells seem to actively use the glycolytic pathway for ATP generation, even in the presence of oxygen. Such increase of aerobic glycolysis in cancer cells is known as the Warburg effect [1]. In addition to its role in producing ATP, the

Correspondence: Peng Huang, Tel: +1-713-834-6044; Fax: +1-713-834-6084, phuang@mdanderson.org.
*These three authors contributed equally to this work.

(Supplementary information is linked to the online version of the paper on the *Cell Research* website.)

glycolytic pathway may also provide important metabolic intermediates to be used for making biomass (nucleic acids, proteins, lipids) needed for cell growth and proliferation [2]. The increase in glucose uptake and utilization represents an important metabolic feature of cancer cells, and is clinically relevant since the majority of human cancers exhibit significant increase in glucose uptake *in vivo*, which can be readily detected by fluorodeoxy glucose-positron emission tomography (FDG-PET), an imaging method used in cancer diagnosis [3, 4]. Despite these long-standing observations, the exact molecular mechanisms responsible for the Warburg effect still remain unclear.

Several molecules, including HIF-1α, c-Myc, and Akt, have been suggested to play important roles in promoting glycolysis and thus may be involved in "metabolic reprogramming" in the cancer cells [5, 6]. Recent studies suggest that oncogenic transformation by the K-ras oncogene may also significantly alter cellular metabolism, including suppression of mitochondrial respiration [7] and increased generation of reactive oxygen species [8]. However, the mechanisms by which Ras induces mitochondrial dysfunction and its effect on energy metabolism and redox status remain poorly understood [9–11]. Since aberrant activation of K-ras by mutations such as K-ras^{G12V} is frequently observed in human cancers, especially in pancreatic cancer where the vast majority of the malignant cells exhibit constitutive activation of K-ras [12, 13], it is important to evaluate the detailed metabolic changes induced by aberrant K-ras activation and the underlying biochemical and molecular mechanisms. A recent study showed that transformation of mouse fibroblasts by K-ras led to a decrease in mitochondrial complex I activity through a yet unknown mechanism [14]. In the current study, we established a doxycycline-inducible K-ras^{G12V} expression cell system, which enables control of K-ras^{G12V} expression in human embryonic kidney cells (HEK293) under defined experimental conditions to allow a precise time-course study of the K-ras-induced metabolic changes in correlation with the changes in other cellular and molecular events. The use of this experimental system enabled us to identify a key molecular player that seems essential to maintain the metabolic changes in K-ras-transformed cells.

Results

Induction of K-ras^{G12V} expression leads to mitochondrial dysfunction

To evaluate the potential role of oncogenic K-ras in causing "respiratory injury" as a metabolic symptom of the Warburg effect [15], we established a tetracycline-inducible K-ras^{G12V} expression cell system (designated as T-Rex/K-ras cells) to directly test if induction of K-ras^{G12V} expression might alter mitochondrial function. As shown in Figure 1A, addition of doxycycline to the culture medium induced a time-dependent expression of K-RAS protein in T-Rex/K-ras cells, detectable as early as 12 h. This oncogene expression caused a rapid decrease in mitochondrial transmembrane potential ($\Delta\Psi_m$), which was also detectable at 12 h (Figure 1B and 1C). Treatment of HEK293 cells harboring the control vector (T-Rex/vector only) with doxycycline under identical conditions did not cause any change in $\Delta\Psi_m$ (Figure 1B), suggesting that the alteration in mitochondrial function observed in K-ras^{G12V} cells was due to the expression of the oncogene, not due to doxycycline *per se*. We then used transmission electron microscopy and fluorescence microscopy to analyze the potential changes in mitochondrial morphology and ultrastructure after K-ras^{G12V} induction. Mitochondrial alterations such as swollen and pale matrix were observed 16 h after induction of K-ras^{G12V} expression, and the cristae became disorganized in cells after long-term (over 1 month) continuous K-ras^{G12V} induction (Supplementary information, Figure S1A). Staining cells with MitoTracker Red revealed no obvious change in mitochondrial mass. However, the normal mitochondrial network clusters seen in the normal cells were disrupted after 48 h of K-ras^{G12V} induction, as evidenced by the

appearance of aberrant dot-shaped mitochondria lacking the normal network connection (Supplementary information, Figure S1B).

One striking change in mitochondrial function observed in cells expressing K-ras^{G12V} was the significant reduction in mitochondrial respiratory chain activity, as evidenced by a substantial decrease in oxygen consumption (Figure 1D). Approximately a 50% decrease in mitochondrial respiration was detected at 12 h after K-ras^{G12V} induction, and further suppression was observed at 24 h (Figure 1E). Polymerase chain reaction (PCR) analysis of mitochondrial DNA (mtDNA) in the K-ras^{G12V}-expressing cells revealed no loss of mtDNA in all segments tested (D-loop, ND4, COII) (Figure 1F), suggesting that the mitochondrial alterations induced by K-ras^{G12V} were not due to a loss of mitochondrial genetic materials. Interestingly, despite these changes in mitochondrial function, no significant cell death was detected at 48 h, and a small portion of cells became apoptotic at 72 h, as detected by annexin-V/PI double staining and flow cytometry analysis (Figure 1G).

Inhibition of mitochondrial respiratory chain complex-I by K-ras^{G12V}

To further investigate the biochemical and molecular basis for K-ras^{G12V}-induced mitochondrial dysfunction, we used specific inhibitors of mitochondrial respiratory complexes in conjunction with proper metabolic substrate supplement and oxygen consumption assay to determine which complex activity might be affected by K-ras^{G12V} expression. The experimental rationale is illustrated in the top panel of Figure 2A. The overall oxygen consumption at complex IV reflects the combined electron transport activities from both complex I→CoQ→III→IV and complex II→CoQ→III→IV. In the presence of the complex I-specific inhibitor rotenone [16, 17] and the complex II substrate succinate (digitonin was also added to make the biological membranes permeable to succinate), the oxygen consumption rate would represent the maximal activity of complex II→CoQ→III→IV. As shown in the lower panel of Figure 2A, the control cells (Tet/off) exhibited a high overall respiratory activity with an oxygen consumption rate of 14.5 nmol/ml/min. The presence of rotenone (100 nM) almost completely suppressed this respiration (indicated by the flat segment of the respiratory curve between 6–12 min), suggesting that most of the electron transport activity was from complex I in the cells without K-ras^{G12V} expression. Addition of the complex II substrate succinate to the rotenone-treated cells resulted in a resumption of oxygen consumption at the rate of 6.6 nmol/ml/min, which reflected the maximal activity of the complex II→CoQ→III→IV segment of the respiratory chain in the control cells. Strikingly, in cells with K-ras^{G12V} expression (Tet/on, 48 h), the overall respiratory activity was 4.3 nmol/ml/min, approximately 30% of the Tet/off cells (14.5 nmol/ml/min). Addition of rotenone to the Tet/on cells caused a slight further decrease in oxygen consumption as evidenced by the flattened curve segment (6–12 min). The supplement of the complex II substrate succinate led to a substantial increase in oxygen consumption rate to 7.5 nmol/ml/min, a level that was slightly higher than that of the Tet/off cells under the same assay conditions (6.6 nmol/ml/min). These data together suggest that the site of respiratory defect in the cells expressing K-ras^{G12V} was at complex I, whereas the function of the respiratory chain segment between complex II and complex IV appeared normal or slightly upregulated. Repeated biochemical analyses in cells with K-ras^{G12V} expression either for 24 h or for 48 h consistently revealed the same pattern of respiratory suppression at complex I (Figure 2B).

We then used a panel of antibodies against the representative components of each mitochondrial respiratory complex to examine if there was any change in the protein levels of the respiratory chain molecules. As shown in Figure 2C, the protein level of the 20-kD component of complex I (a nuclear DNA-encoded protein) was significantly decreased at 24 h and remained low at 48 h, suggesting a destabilization of complex I. Because the 20-kD protein was not decreased at 12 h while respiratory function was already suppressed at this

early time, it is likely that the expression of K-ras^{G12V} might first impact the respiratory function of complex I by its rapid translocation to the mitochondria inner membrane (see below) and cause a dysfunction of the electron transport chain associated with the inner membranes. The dysfunctional complex I subsequently became destabilized. Interestingly, the expression of the 30-kD subunit of mitochondrial respiratory chain complex II (a nuclear DNA-encoded protein) was upregulated (Figure 2C), suggesting a possible cellular response to compensate for the loss of complex I activity. This was also consistent with the slight increase in complex II→IV activity observed in the functional analysis (Figure 2A). In addition, there was an activation of Akt, as demonstrated by the increase of phosphorylation at Ser473 after K-ras^{G12V} induction (Figure 2C), consistent with our previous observations that mitochondrial dysfunction caused Akt activation to promote cell survival [18].

K-ras-induced mitochondrial dysfunction is associated with increased ROS generation and elevated glycolytic activity

Because mitochondrial respiratory chain is a site of reactive oxygen species (ROS) production and K-ras^{G12V} causes respiratory dysfunction, we tested possible changes in ROS generation after K-ras^{G12V} expression. As shown in Figure 2D, K-ras^{G12V} induction by doxycycline (20 ng/ml) caused a significant increase in ROS, while the same concentration of doxycycline did not alter the ROS level in the control cells harboring the empty vector (data not shown), indicating that the increase of ROS production was not due to doxycycline. Figure 2E showed that K-ras^{G12V} activation induced a rapid increase in ROS generation in a time-dependent manner, which was detectable at 12 h and further increased as the time prolonged. Interestingly, the protein levels of two major antioxidants SOD2 and catalase were decreased after K-ras^{G12V} induction (Figure 2C), and the expression of SOD2 mRNA was significantly increased after K-ras^{G12V} activation (Supplementary information, Figure S2B), suggesting that the decrease in SOD2 protein was not due to a reduction in transcription.

As the time of K-ras^{G12V} expression prolonged, the cells began to exhibit metabolic adaptation to the mitochondrial dysfunction by increasing glycolytic activity, increase evidenced by a significant in glucose uptake and lactate production at 72 h (Figure 2F). However, oxygen consumption was only partially recovered from 28% at 24 h to 40%–45% at 72 h (compared to the respiration rate in the control cells without K-ras^{G12V} expression). The temporal relationship between the early mitochondrial dysfunction and the relatively late increase in glycolytic activity suggests that the upregulation of glycolysis was likely a cellular response to the metabolic stress due to decrease in mitochondrial respiration induced by K-ras^{G12V}.

Translocation of K-RAS protein to mitochondria and its role in causing mitochondrial dysfunction

Previous studies suggest that RAS protein may translocate from the plasma membrane to intracellular compartments including mitochondria [19–21]. We postulated that mitochondrial dysfunction observed in the K-ras^{G12V}-expressing cells might involve the physical presence of K-RAS protein in the mitochondria to interfere with the respiratory activity. To test this possibility, mitochondria were isolated from the cells before and after K-ras^{G12V} induction, and the presence of K-RAS protein in the isolated mitochondria was revealed by western blot analysis. As shown in Figure 3A, doxycycline induced a rapid appearance of K-RAS protein in the mitochondrial fraction at 12 h. Blotting of mitochondrial Hsp60 showed an equal loading of mitochondrial proteins from the Tet/on and Tet/off cells. The lack of tubulin in the mitochondrial fractions suggests that there was no significant cytosolic contamination in the isolated mitochondria (Figure 3A). To further determine if the K-RAS protein was localized on the surface of the mitochondria or inside

the organelle, we used trypsin to digest the proteins on the mitochondrial surface, and then examined whether such digestion causes a degradation of K-RAS protein in the mitochondrial fraction. Under these experimental conditions, proteins associated with the outer mitochondrial membrane facing outward would be cleaved decrease of by trypsin, while the protein in the inner compartment would be protected. As illustrated in Figure 3B, incubation of isolated mitochondria from the Tet/on cells at 4 °C, 24 °C, or 37 °C led to cleavage of about 40% of the K-RAS protein associated mitochondria, while 60% of the K-RAS protein remained intact under all digestion conditions including 37 °C, suggesting that a major portion of this protein was inside the mitochondria. Hexokinase II (HKII, a protein known to be associated with mitochondria on the outer membrane) and cytochrome c (located inside the mitochondria) were used as the controls for trypsin digestion. As shown in Figure 3B, HKII was completely degraded by the trypsin, while cytochrome c remained undigested under the same treatment conditions. We then used RIPA buffer containing detergents (0.1% SDS and 1% Triton X-100) to disrupt mitochondrial membranes and extract proteins from the isolated mitochondria. After removal of SDS and salts from the protein extracts by buffer exchange using the YM-10 column (Microcon), trypsin digestion led to a complete disappearance of the intact K-RAS protein band (Supplementary information, Figure S3), further suggesting that a large portion of the K-RAS protein was indeed protected by the mitochondrial membranes.

Confocal microscopic analysis was then used to confirm the translocalization of K-RAS protein to the mitochondria. Mitochondria were stained with MitoTracker Red and K-RAS protein was detected using FITC-conjugated antibody with green fluorescent signal. Under these experimental conditions, mitochondrial localization of K-RAS would show as a yellow signal due to the overlap of green and red fluorescence. As shown in Figure 3C, the HEK293 cells exhibited a barely detectable weak K-RAS background signal (green) before doxycycline induction. After induction with doxycycline for 12 h, K-RAS protein expression (green signal) was highly induced. A large portion of the K-RAS protein accumulated in the mitochondria and appeared as yellow spots.

To evaluate the role of K-RAS translocation to mitochondria in causing mitochondrial dysfunction, we tested if a blockage of such translocation in the Tet/on cells would prevent the induction of changes in mitochondrial transmembrane potential. Because protein kinase C (PKC) is known to facilitate the translocation of K-RAS from plasma membrane to mitochondria [20], we used the PKC inhibitor H-7 to test its effect on K-RAS translocation to mitochondria and the functional consequence. As shown in Figure 3D, there was a strong K-RAS band in the mitochondrial fraction 12 h after doxycycline induction (without H-7), and this was associated with a significant transmembrane potential $\Delta\Psi m$ (Figure 3E). Addition of 25 μM H-7 largely blocked the translocation of K-RAS to mitochondria (Figure 3D) and effectively prevented the loss of $\Delta\Psi m$ (Figure 3E), suggesting that the translocation of K-RAS protein to mitochondria was important in causing mitochondrial dysfunction.

Because the dissipation of the transmembrane potential may be caused by a sustained opening of the mitochondrial permeability transition pore (MPTP) consisting of voltage-dependent-anion-channel (VDAC), adenine-nucleotide-translocator (ANT) and cyclophilin D (CyD) [22, 23], we used cyclosporin A (CysA), a CyD inhibitor that prevents the interaction between CyD and ANT [22], to test its effect on K-ras^{G12V}-induced loss of mitochondrial transmembrane potential. As shown in Figure 3F and 3G, 5 μM CysA completely prevented the loss of transmembrane potential caused by K-ras^{G12V} expression, suggesting that the CysA-sensitive MPTP was involved in K-ras^{G12V}-induced mitochondrial dysfunction.

Reversibility of K-ras^{G12V}-induced mitochondrial dysfunction and ROS generation

We next asked whether the continuous K-ras^{G12V} expression is required for sustaining the suppression of mitochondrial function and maintaining elevated ROS generation. K-ras^{G12V} was first induced for 48 h, and then doxycyclin was removed and cells were cultured in fresh medium for additional 3 days (without doxycycline). As shown in Figure 4A, K-RAS protein decreased substantially within 24 h after doxycycline removal, and completely disappeared at 48 h. Concurrently, there was a time-dependent recovery of expression of SOD2 and catalase, which were originally suppressed when K-ras^{G12V} was induced (Figure 4A). Analysis of cellular ROS by flow cytometry revealed that the increase of ROS in the K-ras^{G12V}-expressing cells was reduced back to almost normal level after doxycyclin withdrawal (Figure 4B). Importantly, the mitochondrial transmembrane potential in the Tet/on cells was almost completely restored to the normal level (comparable to the Tet/off control) 2 days after doxycycline withdrawal (Figure 4C). Under the influence of K-ras signal and ROS stress, the Tet/on cells exhibited certain stress morphology such as rounding up and partial detaching from the culture surface (Figure 4D, middle panel). Removal of doxycycline for 2 days led to the reversal of cell morphology to the normal appearance, similar to that of the Tet/off control cells (Figure 4D).

Long-term induction of K-ras^{G12V} led to metabolic adaptation and increase in tumorigenesis

Since the induction of K-ras^{G12V} expression caused an acute mitochondrial dysfunction leading to significant metabolic alterations manifested by an increase in glycolysis and ROS stress, we further evaluated the long-term effect of K-ras^{G12V} expression on glycolytic metabolism and redox status of the cells. As shown in Figure 5A, a long-term (>1 month) induction of K-ras^{G12V} expression by doxycycline (20 ng/ml) resulted in a stable metabolic adaptation phenotype, characterized by a low mitochondrial respiration (approximately 60% oxygen consumption compared to the Tet/off control cells) and high glycolytic activity, evidenced by increased glucose uptake and elevated lactate generation. Western blot analysis showed that such induction of K-ras^{G12V} and mitochondrial dysfunction was associated with Akt activation, evidenced by increased phosphorylation of Akt at S473 without change in total Akt protein level (Figure 5B). This was consistent with our previous observation that mitochondrial dysfunction caused Akt activation [18]. Hexokinase-2 (HKII), a key glycolytic enzyme regulated by the Akt pathway, was significantly increased in the Tet/on cells (Figure 5B). This might contribute to the upregulation of glycolysis in these cells. Interestingly, mitochondrial mass was moderately increased after long-term K-ras activation (Figure 5C), likely reflecting a compensatory biogenesis in response to the functional suppression by K-ras^{G12V}. The continuous induction K-ras^{G12V} for over a month also led to a moderate but sustained increase in cellular ROS (Figure 5D). Quantitation of cellular glutathione (GSH), a major cellular antioxidant, revealed a slight increase at 48 h of K-ras^{G12V} induction and a significantly higher level in the long-term Tet/on cells (Figure 5E), suggesting an adaptive upregulation of GSH synthesis in response to the sustained ROS stress caused by K-ras^{G12V}.

The above observations suggest that the expression of K-ras^{G12V} caused mitochondrial dysfunction and an increase in ROS generation. In response, cells upregulated glycolysis to compensate energy metabolism, and increased GSH synthesis to counteract ROS stress. This metabolic adaptation was especially prominent in the long-term Tet/on cells. We suspected that such adaptation might be important for the transformed cells to proliferate and form tumor *in vivo*. To test this possibility, we first treated the T-Rex K-ras^{G12V} cells with or without doxycycline in culture for over a month to allow sufficient time for metabolic adaptation, and then compared their ability to form colonies in soft agar, using an anchorage-independent colony formation assay. As shown in Figure 5F, the Tet/off cells

exhibited little ability to form colonies in soft agar, whereas the long-term Tet/on cells readily formed colonies. To further compare their ability to form tumor *in vivo*, we inoculated T-Rex/K-ras cells with or without long-term pre-induction of K-ras^{G12V} into nude mice, and observed tumor formation and tumor growth for 2 months. To minimize the influence of individual variation, each mouse was inoculated with long-term Tet/on cells subcutaneously on the left flank and the Tet/off cells on the right flank. All mice received doxycycline during the 2-month observation period. As shown in Figure 5G and 5H, the cells with long-term pre-induction of K-ras *in vitro* showed higher tumor formation incidence (4/10) than those without pre-induction (1/10), and the tumor xenografts from the pre-induced cells exhibited significantly higher growth rate. These data suggest that long-term induction of K-ras^{G12V} expression *in vitro* allows metabolic adaptation to promote the ability of the transformed cells to form tumors *in vivo*.

Discussion

Increased aerobic glycolysis in cancer cells is known as the Warburg effect, which has been observed in a variety of malignant tumors. This metabolic alteration is considered as a characteristic biochemical symptom of cancer cells and seems to be associated with mitochondrial dysfunction or respiration injury [1]. The association between deregulation of mitochondrial function and oncogenic transformation has been reported in different experimental models including yeast [24], mouse [7, 8] and human fibroblasts[9]. It has been known for some time that oncogenic transformation by Ras could lead to mitochondrial dysfunction [7], although the detailed molecular and biochemical events linking Ras activation and the changes in energy metabolism still remain to be elucidated. In the current study, we established a tetracycline-inducible K-ras^{G12V} expression system to examine the detailed metabolic changes after induction of K-ras^{G12V} and to evaluate the temporal relationship between the oncogene expression and several key metabolic parameters. Our study showed that expression of K-ras^{G12V} protein resulted in a significant decrease in mitochondrial respiration, accompanied by a decrease of mitochondrial transmembrane potential and an increase of ROS generation, detectable as early as 12 h after doxycycline induction. Fluorescent and electron microscopy also revealed alterations in mitochondrial morphology 48 h after K-ras induction. It seems that aberrant activation of the K-ras oncogene is able to cause rapid dysfunction of mitochondria leading to structural changes.

Although the expression of K-ras^{G12V} consistently caused both rapid suppression of mitochondrial respiration and a decrease of mitochondrial transmembrane potential ($\Delta\Psi_m$), the mechanistic link between these two parameters (respiration and $\Delta\Psi_m$) is still unclear. Interestingly, in the experiments using CysA to block K-ras^{G12V}-induced loss of $\Delta\Psi_m$, we observed that such preservation of $\Delta\Psi_m$ did not prevent K-ras^{G12V}-induced suppression of respiration (data not shown). These data seem to suggest that inhibition of the mitochondrial respiratory chain activity may be a primary event caused by K-ras^{G12V}, whereas the loss of transmembrane potential may be functionally a downstream event. The MPTP, consisting of VDAC, ANT, and CyD, is known to play an important role in maintaining $\Delta\Psi_m$ and its opening would lead to dissipation of $\Delta\Psi_m$ [22, 25]. Binding of CysA to CyD effectively suppressed the opening of MPTP and thus prevented loss of $\Delta\Psi_m$, but this was unable to reverse the inhibition of respiratory chain activity, indicating that K-ras^{G12V} might directly affect the mitochondrial respiratory chain function rather than through disrupting mitochondrial membrane permeability.

By using a combination of specific inhibitors of electron transport complexes and proper subtract supplement, we showed that complex I was likely the primary site in the respiratory chain impacted by K-ras^{G12V}, although the exact peptide component that interacts with K-ras^{G12V} protein still remains unclear at the present time. The decrease in the 20-kD protein

shown in Figure 2C likely reflected the overall disruption of complex I, leading to instability of its protein components at the relatively later time points (24–48 h), since the suppression of respiration occurred at an earlier time (12 h) without detectable loss of the 20-kD protein. Interestingly, there seemed to be a compensatory upregulation of complex II, as evidenced by the increased expression of the 30-kD component (a nuclear-encoded protein). Analysis of the representative components of other respiratory chain complexes using commercially available antibodies showed no significant changes in complex III-IV. In a separate study, we used a SILAC (stable isotope labeling with amino acids in cell culture)-based mass spectrometry method to analyze possible changes in mitochondrial respiratory chain components, and found that many of the complex I components including NDUFA2, NDUFA4, NDUFA5, NDUFA11, NDUFA12, NDUFA13, NDUFB4, NDUFB6, NDUFB7 were substantially decreased (30%–50%) at 24 h and 48 h (data not shown). These data together suggest that translocation of K-RAS protein to mitochondria might cause a disruption of complex I, resulting in an increased degradation of its protein components.

Several studies suggest that the RAS protein may be physically associated with mitochondria [19–21], although the exact localization of the RAS protein in the mitochondria still remains to be determined. Our study using confocal microscopy analysis suggested that a portion of K-RAS protein was indeed localized to the mitochondria. Some of the mitochondria-associated K-RAS proteins might be within the mitochondria since they were protected from trypsin digestion. The observation that blocking RAS translocation to the mitochondria by H-7 prevented the loss of transmembrane potential in the K-ras^{G12V}-expressing cells (Figure 3D and 3E) seems to suggest that the localization of K-RAS protein to mitochondria might contribute to the inhibition of mitochondrial respiratory chain. However, the exact role of K-RAS protein localization to the mitochondria in causing suppression of mitochondrial respiration still remains unclear. One possibility would be that K-RAS protein in the mitochondria might interact with a respiratory chain component and interfere with its function. Another possibility might involve NADPH oxidase (NOX)-mediated generation of ROS, which could then impact the redox-sensitive mitochondrial respiratory chain components. In fact, it has been shown that K-ras-induced transformation involves activation of NOX and increased generation of ROS [26–28]. It is also possible that K-RAS might interact with a mitochondrial membrane-associated molecule and thus decrease the transmembrane potential and affect respiratory function. Obviously, further studies are needed to test these possibilities.

We found that K-ras induction is associated with a significant increase of ROS production. Since mitochondrial electron transport chain is a site of ROS generation, we speculate that the K-ras-induced mitochondrial dysfunction might increase the leakage of electrons, which then react with molecular oxygen to form superoxide. However, it is possible that other mechanisms may be involved in this ROS increase. For instance, recent studies showed that NOX plays an important role in generation of superoxide and in mediating Ras-induced transformation [26–28]. Indeed, we also observed the induction of K-ras^{G12V} expression in the T-Rex/K-ras cells was associated with increased expression of NOX components (data not shown). Thus, it is possible that both mitochondrial dysfunction and elevated NOX activity may contribute to ROS increase induced by K-ras^{G12V}. Further study is required to test this possibility and to determine the relative contribution of mitochondrial respiratory chain and NOX in ROS generation under these conditions.

One major finding of this study was that the expression of K-ras^{G12V} led to a significant increase in glycolytic activity. The elevated glycolysis appeared to be a compensatory response to mitochondrial dysfunction, since mitochondrial respiratory suppression occurred 12 h after K-ras^{G12V} induction, whereas increased glycolysis was a much later event (72 h). In cells with compromised mitochondrial respiration and thus lower ATP generation through

oxidative phosphorylation, upregulation of glycolysis is important to generate additional ATP to make up for the loss of energy generation in the dysfunctional mitochondria. Interestingly, the mitochondrial mass in the long-term Tet/on cells was increased (Figure 5C), but these cells still exhibit lower respiration and higher glycolysis, suggesting that the increase in mitochondrial mass was unable to completely compensate for the functional defect in ATP synthesis and thus the cells still required active glycolysis. Indeed, oxygen consumption remains low in the long-term Tet/on cells despite the increased mitochondrial mass. Such defect in mitochondrial function would render the cells more dependent on glycolysis. Consistently, a previous study showed that several enzymes involved in the glycolytic pathway were overexpressed in human pancreatic adenocarcinoma tissues compared to the non-malignant pancreatic tissues [29].

It is of interest to note that a long-term pre-induction of K-ras^{G12V} expression *in vitro* substantially enhanced the ability of these transformed cells to form colonies in soft agar and to form tumors *in vivo*. It is likely that the long-term pre-induction of K-ras^{G12V} would allow sufficient time for the cells to undergo metabolic adaptation, during which the cells upregulated glycolysis and enhanced GSH synthesis. The increase in glycolytic capacity would enable the cells to generate sufficient ATP and metabolic intermediates for the cells to proliferate in the hypoxic tissue microenvironment. Since generation of ATP through glycolysis does not require oxygen, this metabolic property may be important for tumor growth *in vivo*, where hypoxia is frequently present in the tissue environment. Similarly, cells within the colonies in soft agar may also experience local hypoxia due to the gel barrier that retards oxygen diffusion. The increased ability of long-term K-ras^{G12V}-expressing cells to form colonies in soft agar and form tumor *in vivo* (Figure 5F–5H) supports this notion. At the molecular level, activation of Akt may contribute to the enhancement of glycolysis through its upregulation of HKII (Figure 5B). This is consistent with our previous observation that mitochondrial dysfunction could lead to Akt activation by a redox-mediated inactivation of PTEN, which is a negative regulator of Akt [18]. The well-established roles of Akt in promoting cell survival and enhancing glycolysis may significantly contribute to the increased tumorigenicity of the K-ras^{G12V}-transformed cells.

In summary, our study showed that induction of K-ras^{G12V} expression caused mitochondrial dysfunction manifested by a rapid decrease in respiration, a reduction in mitochondrial transmembrane potential, and an increase in generation of ROS. The translocation of K-RAS protein to mitochondria was associated with these biochemical alterations. Suppression of the respiratory chain complex-I seemed to be a major event, which was associated with a destabilization of the complex I components in the K-ras^{G12V}-expressing cells. Increased glycolysis and elevated synthesis of GSH were two major metabolic adaptation events in response to mitochondrial dysfunction induced by K-ras^{G12V}. These adaptations would enable the cells to generate sufficient energy to compensate for the loss of ATP generation in the mitochondria and to increase antioxidant capacity to counteract the elevated ROS. As such, these metabolic changes may be important for the survival of the Ras-transformed cells, and could be exploited for therapeutic purpose. For instance, inhibition of glycolysis and abrogation of the GSH antioxidant system might be effective strategies to kill Ras-transformed cancer cells. These possibilities require further study.

Materials and Methods

Vector construction and cell culture

The full-length cDNA containing the K-*ras*^{G12V} gene sequence was constructed into the pcDNA4/TO vector (Invitrogen) at the *Eco*RV restriction site. The resulting pcDNA4/TO-K-*ras*^{G12V} construct was confirmed for correct orientation and reading frame by direct DNA sequencing. HEK293 cells (T-Rex-293 from Invitrogen) pre-transfected with the tet-

repressor vector (pcDNA6/TR) were further transfected with 1.5 μg of pcDNA4/TO-K-*ras*^{G12V} plasmid DNA or the pcDNA4/TO vector-only as a control. Blasticidin (10 μg/ml) and Zeocin (200 μg/ml) were added into cell cultures to select the cell clones stably transfected with both pcD-NA6/TR and pcDNA4/TO-K-*ras*^{G12V}. Stable clones were routinely maintained in Dulbecco's modified Eagle's medium (DMEM) supplemented with 10% fetal bovine serum, 10 μg/ml blasticidin and 200 μg/ml Zeocin. K-ras^{G12V} expression was induced by 20 ng/ml doxycycline and confirmed by western blot analysis. T-Rex cells with long-term induction of K-ras^{G12V} were maintained with 20 ng/ml doxycycline (over 2 months). HPDE cells and HPDE/K-ras^{G12V} cells were cultured in Keratinocyte-SFM medium (GIBCO).

Antibodies and reagents

The following antibodies were used for immunoblotting analyses using standard western blotting procedures: K-ras (Calbiochem), HSP60 (Abcam), β-actin (Calbiochem), tubulin, cytochrome c and AKT (Cell Signaling), SOD2, and HKII (Santa Cruz), complex I 20 kD, and complex II 30 kD (Invitrogen). H-7 and CysA were purchased from Sigma.

Flow cytometry analysis of ROS generation, mitochondria mass and transmembrane potential

Cells were stained with 60 nM MitoTracker Green (Invitrogen) for 60 min to measure the mitochondrial mass, with 5 μM DCF-DA (60 min) to detect cellular ROS, and with 1 μM rhodamine-123 (60 min) to evaluate the mitochondrial transmembrane potential. Analysis was performed using a FACScan flow cytometer (Becton Dickinson).

Cellular GSH analysis

A glutathione assay kit (Cayman Chemical Co., Ann Arbor, MI, USA) was used to measure total cellular GSH as described [30]. Briefly, cell extracts were prepared by sonication and deproteination. The level of total GSH was detected by measuring the product of glutathionylated DTNB by UV spectrophotometer at 405 nm. The cellular GSH contents were calculated using the standard curve generated in parallel experiments and expressed as nmoles/10^6 cells. Cell number and median cell volume were quantified using a Coulter ® Z_2 particle count and size analyzer.

Determination of glycolytic activity

The cellular glycolytic activity was evaluated by measuring lactate production, glucose uptake and oxygen consumption rate. To determine the cellular lactate production, cells in exponential growth phase were washed and incubated with fresh medium for the indicated times. Culture media were removed for the analysis of lactate content using a lactate analyzer with a linear range of standard lactate concentrations according to the manufacturer's instruction (Roche, Mannheim, Germany). Cellular glucose uptake was measured by incubating cells in glucose-free DMEM for 2 h before incubation with 0.2 Ci/ml [^{3}H]2-deoxyglucose (specific activity, 40 Ci/mmol) for 1 h. After the cells were washed with ice-cold PBS, the radioactivity in the cell pellets was quantified by liquid scintillation counting.

Determination of oxygen consumption

Five million cells were resuspended in 1 ml of fresh warm medium pre-equilibrated with 21% oxygen and placed in the sealed respiration chamber equipped with a thermostat control, a micro-stirring device, and a Clark-type oxygen electrode disc (Oxytherm, Hansatech Instrument, Cambridge, UK). The oxygen content in the cell suspension medium was constantly monitored for 20 min and oxygen consumption rate was recorded. To

measure mitochondrial respiratory chain complex I and II activity, 5 million cells were resuspended in respiration buffer containing 20 mM HEPES pH 7.4, 10 mM $MgCl_2$ and 250 mM sucrose. At 6 min after the recording, 100 nM rotenone was added to suppress the activity of complex I. At 10 min, 30 μg/ml digitonin was added to make the cell membrane permeable to complex II substrate succinate. At 12 min, 5 μM succinate was added to record the activity of complex II.

DNA isolation and PCR

Total DNA from T-Rex cells was isolated using DNeasy blood and tissue kit (QIAGEN) and amplified under standard PCR conditions using mitochondrial-specific PCR primers for D loop, ND4, COXII and β-actin as described previously [31].

Immunofluorescence and confocal microscopy

Cells before and after K-ras induction were cultured on sterilized glass slide covers until 70%–80% confluence and incubated with 200 nM MitoTracker Red for 1 h. Cells were washed with fresh warm DMEM medium for 5 min twice and fixed with 3.7% paraformaldehyde in medium at 37 °C for 15 min, washed with PBS, and then incubated with 5% BSA for 30 min at room temperature (RT). The samples were incubated at RT for 3 h with mouse anti-K-ras, washed, and then incubated with FITC-labeled anti-mouse antibody for 1 h. Finally, samples were stained with 400 ng/ml DAPI in PBS for 5 min at RT. The slide covers were mounted on glass slides with Vectashield® mounting medium (Vector Laboratories, CA, USA). Images were taken by NIKON Eclipse TE2000 confocal microscope and analyzed by using Nikon EZ-C1 software.

Soft agar and tumorigenecity

HEK293 cells before and after long-term K-ras induction (4×10^4 cells/well) were seeded in 0.35% agarose over a layer of 0.7% agarose in a six-well plate. After incubation for 15 days, colonies were stained overnight with p-iodonitroterazolium violet and colonies were counted. 3×10^6 cells before and after long-term K-ras induction were inoculated subcutaneously on the left and right flanks of five nude mice. All mice received doxycycline injection (10 mg/kg) every other day on day 1–13 and daily on day 15–60. The mice were monitored for tumor growth and body weight.

Supplementary Material

Refer to Web version on PubMed Central for supplementary material.

Acknowledgments

We thank Kenneth Dunner for expert technical assistance in electron microscopic analysis. This work was supported in part by grants CA085563, CA100428 and CA109041 from the National Institutes of Health.

References

1. Warburg O. On the origin of cancer cells. Science. 1956; 123:309–314. [PubMed: 13298683]
2. Vander Heiden MG, Cantley LC, Thompson CB. Understanding the Warburg effect: the metabolic requirements of cell proliferation. Science. 2009; 324:1029–1033. [PubMed: 19460998]
3. Kaira K, Endo M, Abe M, et al. Biologic correlates of (1) F-FDG uptake on PET in pulmonary pleomorphic carcinoma. Lung Cancer. 2011; 71:144–150. [PubMed: 20646779]
4. Vergez S, Delord JP, Thomas F, et al. Preclinical and clinical evidence that Deoxy-2-[18F]fluoro-D-glucose positron emission tomography with computed tomography is a reliable tool for the detection of early molecular responses to erlotinib in head and neck cancer. Clin Cancer Res. 2010; 16:4434–4445. [PubMed: 20660574]

5. Vafa O, Wade M, Kern S, et al. c-Myc can induce DNA damage, increase reactive oxygen species, and mitigate p53 function: a mechanism for oncogene-induced genetic instability. Mol Cell. 2002; 9:1031–1044. [PubMed: 12049739]
6. Kim JW, Dang CV. Cancer's molecular sweet tooth and the Warburg effect. Cancer Res. 2006; 66:8927–8930. [PubMed: 16982728]
7. Chiaradonna F, Gaglio D, Vanoni M, Alberghina L. Expression of transforming K-Ras oncogene affects mitochondrial function and morphology in mouse fibroblasts. Biochim Biophys Acta. 2006; 1757:1338–1356. [PubMed: 16987493]
8. Chiaradonna F, Sacco E, Manzoni R, et al. Ras-dependent carbon metabolism and transformation in mouse fibroblasts. Oncogene. 2006; 25:5391–5404. [PubMed: 16607279]
9. Ramanathan A, Wang C, Schreiber SL. Perturbational profiling of a cell-line model of tumorigenesis by using metabolic measurements. Proc Natl Acad Sci USA. 2005; 102:5992–5997. [PubMed: 15840712]
10. Vizan P, Boros LG, Figueras A, et al. K-ras codon-specific mutations produce distinctive metabolic phenotypes in NIH3T3 mice [corrected] fibroblasts. Cancer Res. 2005; 65:5512–5515. [PubMed: 15994921]
11. Biaglow JE, Cerniglia G, Tuttle S, et al. Effect of oncogene transformation of rat embryo cells on cellular oxygen consumption and glycolysis. Biochem Biophys Res Commun. 1997; 235:739–742. [PubMed: 9207231]
12. Bos JL. ras oncogenes in human cancer: a review. Cancer Res. 1989; 49:4682–4689. [PubMed: 2547513]
13. Bardeesy N, DePinho RA. Pancreatic cancer biology and genetics. Nat Rev Cancer. 2002; 2:897–909. [PubMed: 12459728]
14. Baracca A, Chiaradonna F, Sgarbi G, et al. Mitochondrial Complex I decrease is responsible for bioenergetic dysfunction in K-ras transformed cells. Biochim Biophys Acta. 2010; 1797:314–323. [PubMed: 19931505]
15. Warburg O. On respiratory impairment in cancer cells. Science. 1956; 124:269–270. [PubMed: 13351639]
16. Degli Esposti M. Inhibitors of NADH-ubiquinone reductase: an overview. Biochim Biophys Acta. 1998; 1364:222–235. [PubMed: 9593904]
17. Chan TS, Teng S, Wilson JX, et al. Coenzyme Q cytoprotective mechanisms for mitochondrial complex I cytopathies involves NAD(P)H: quinone oxidoreductase 1(NQO1). Free Radic Res. 2002; 36:421–427. [PubMed: 12069106]
18. Pelicano H, Xu RH, Du M, et al. Mitochondrial respiration defects in cancer cells cause activation of Akt survival pathway through a redox-mediated mechanism. J Cell Biol. 2006; 175:913–923. [PubMed: 17158952]
19. Wolfman JC, Planchon SM, Liao J, Wolfman A. Structural and functional consequences of c-N-Ras constitutively associated with intact mitochondria. Biochim Biophys Acta. 2006; 1763:1108–1124. [PubMed: 16996152]
20. Bivona TG, Quatela SE, Bodemann BO, et al. PKC regulates a farnesyl-electrostatic switch on K-Ras that promotes its association with Bcl-XL on mitochondria and induces apoptosis. Mol Cell. 2006; 21:481–493. [PubMed: 16483930]
21. Rebollo A, Perez-Sala D, Martinez AC. Bcl-2 differentially targets K-, N-, and H-Ras to mitochondria in IL-2 supplemented or deprived cells: implications in prevention of apoptosis. Oncogene. 1999; 18:4930–4939. [PubMed: 10490827]
22. Grimm S, Brdiczka D. The permeability transition pore in cell death. Apoptosis. 2007; 12:841–855. [PubMed: 17453156]
23. Tsujimoto Y, Shimizu S. Role of the mitochondrial membrane permeability transition in cell death. Apoptosis. 2007; 12:835–840. [PubMed: 17136322]
24. Hlavata L, Aguilaniu H, Pichova A, Nystrom T. The oncogenic RAS2(val19) mutation locks respiration, independently of PKA, in a mode prone to generate ROS. EMBO J. 2003; 22:3337–3345. [PubMed: 12839995]
25. Newmeyer DD, Ferguson-Miller S. Mitochondria: releasing power for life and unleashing the machineries of death. Cell. 2003; 112:481–490. [PubMed: 12600312]

26. Arnold RS, Shi J, Murad E, et al. Hydrogen peroxide mediates the cell growth and transformation caused by the mitogenic oxidase Nox1. Proc Natl Acad Sci USA. 2001; 98:5550–5555. [PubMed: 11331784]
27. Mitsushita J, Lambeth JD, Kamata T. The superoxide-generating oxidase Nox1 is functionally required for Ras oncogene transformation. Cancer Res. 2004; 64:3580–3585. [PubMed: 15150115]
28. Komatsu D, Kato M, Nakayama J, Miyagawa S, Kamata T. NADPH oxidase 1 plays a critical mediating role in oncogenic Ras-induced vascular endothelial growth factor expression. Oncogene. 2008; 27:4724–4732. [PubMed: 18454179]
29. Mikuriya K, Kuramitsu Y, Ryozawa S, et al. Expression of glycolytic enzymes is increased in pancreatic cancerous tissues as evidenced by proteomic profiling by two-dimensional electrophoresis and liquid chromatography-mass spectrometry/mass spectrometry. Int J Oncol. 2007; 30:849–855. [PubMed: 17332923]
30. Trachootham D, Zhou Y, Zhang H, et al. Selective killing of oncogenically transformed cells through a ROS-mediated mechanism by beta-phenylethyl isothiocyanate. Cancer Cell. 2006; 10:241–252. [PubMed: 16959615]
31. Carew JS, Zhou Y, Albitar M, et al. Mitochondrial DNA mutations in primary leukemia cells after chemotherapy: clinical significance and therapeutic implications. Leukemia. 2003; 17:1437–1447. [PubMed: 12886229]

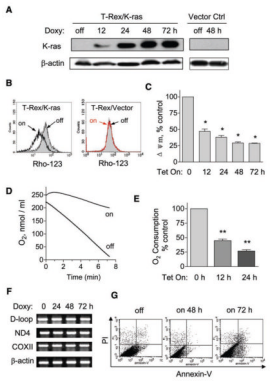

Figure 1.

K-ras^{G12V} activation caused mitochondrial dysfunction. **(A)** 20 ng/ml doxycycline induced ectopic K-ras expression in T-Rex/K-ras cells in a time-dependent manner. The same doxycycline treatment in T-Rex/Vector control cells caused no significant changes. Protein expression of K-ras$_{G12V}$ was detected by immunoblotting with specific antibody for K-ras. β-Actin was used as a loading control. **(B)** Loss of mitochondrial transmembrane potential in T-Rex/K-ras after K-ras induction by doxycycline for 24 h, measured by fluorescent probe Rho-123. The same concentration of doxycycline caused no effect on trans-membrane potential in vector control cells. **(C)** K-ras activation caused a decrease of mitochondrial transmembrane potential in a time-dependent manner. Transmembrane potential levels of induced cells were normalized to the level of cells without induction. **(D)** Oxygen consumption rate of T-Rex-293 cells with (Tet/on) and without (Tet/off) K-ras activation for 24 h. **(E)** K-ras activation inhibited oxygen consumption in a time-dependent manner. **(F)** K-ras activation did not affect mitochondrial DNA contents. **(G)** Effect of K-ras activation on cell viability measured by annexin V-PI assay. Data in **C** and **E** are shown as mean ± SD. $n = 3$, $^{*}P < 0.05$, $^{**}P < 0.01$.

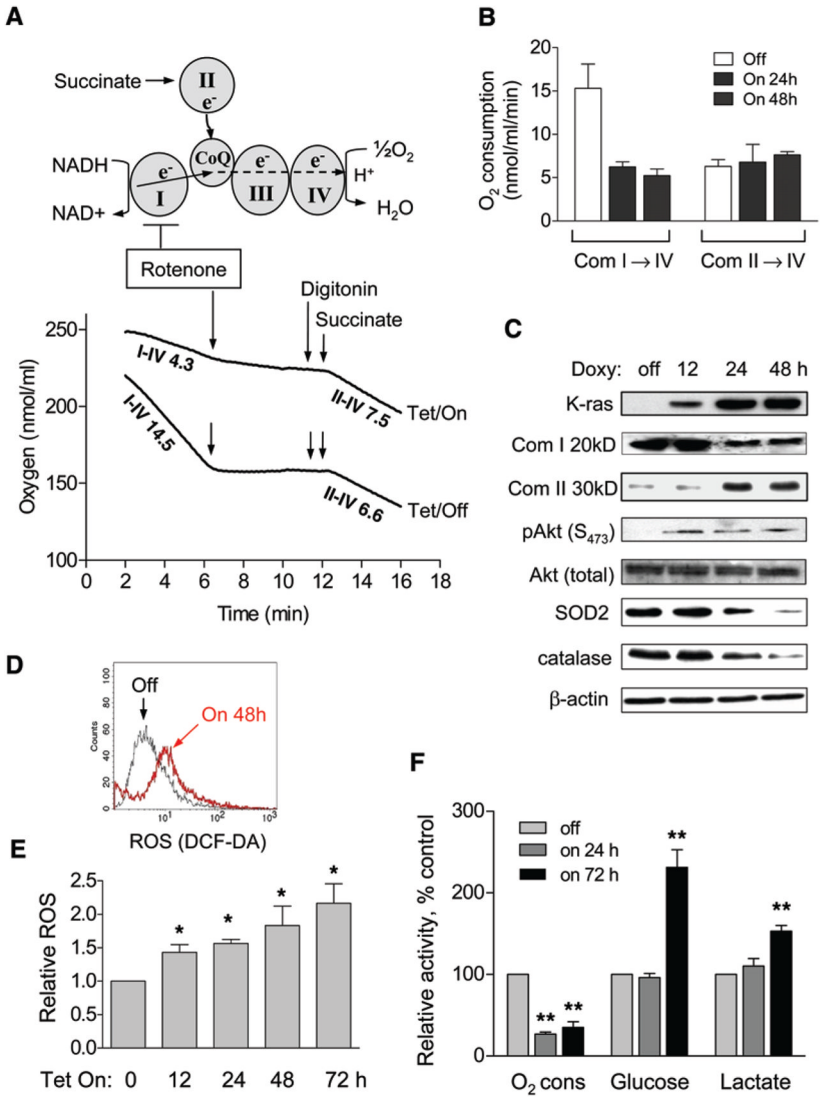

Figure 2.

Mitochondrial dysfunction induced by K-ras^{G12V} activation led to metabolic alterations. **(A)** Experimental rationale of analyzing mitochondrial complex I and II activities and representative oxygen consumption curve of T-Rex-293 cells before and after K-ras induction for 48 h. The numbers indicate oxygen consumption rate (nmol/ml/min) of mitochondrial complex I to IV and II to IV. Arrows indicate the time points when reagents were added. Rotenone: 100 nM; digitonin: 30 μg/ml; succinate: 5 μM. **(B)** Quantitative analysis of oxygen consumption rates of complex I-IV and II-IV after K-ras induction. Data are mean ± SD. $n = 3$, $^{*}P < 0.05$, $^{**}P < 0.01$. **(C)** K-ras^{G12V} induction caused a decrease of complex I 20 kD (Com I 20 kD) subunit and increase of complex II 30 kD (Com II 30 kD) subunit of mitochondrial respiratory chain and increase of phospho-Akt (S_{473}). SOD2 and catalase were also inhibited 24 h after induction. **(D)** K-ras activation for 48 h caused significant increase of ROS production measured by fluorescent probeDCF-DA. **(E)** K-ras activation caused an increase of ROS generation in a time-dependent manner. **(F)** Effect of K-ras activation on oxygen consumption, glucose uptake and lactate production. The metabolic parameters were measured 24 h and 72 h after K-ras induction.

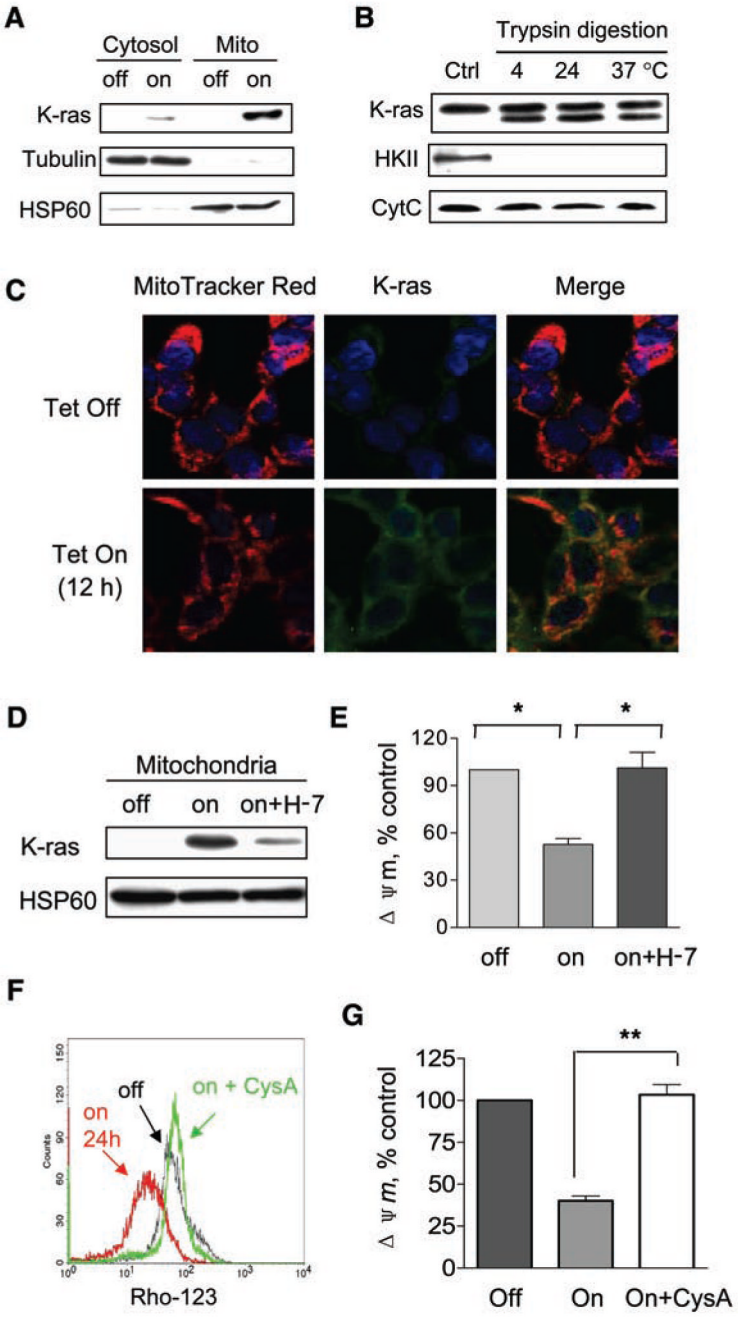

Figure 3.

Translocation of K-RAS protein to the mitochondria and its role in causing mitochondrial dysfunction. **(A)** Mitochondrial fraction was isolated from T-Rex cells before and after doxycycline induction for 12 h. Protein lysates of cytosol and mitochondria (Mito) were analyzed for the presence of K-ras. HSP60 and tubulin were used as mitochondrial and cytosolic markers, respectively. **(B)** Isolated mitochondria from T-Rex cells with K-ras$_{G12V}$ induction (Control) were treated with 100 μg/ml trypsin for 30 min at 4 °C, 24 °C and 37 °C. Western blotting analysis was used to reveal K-ras, hexokinase II (HKII) and cytochrome c. **(C)** Confocal microscopic analysis of the localization of K-ras. HEK293 cells before and after K-ras induction for 12 h were labeled with MitoTracker Red, K-ras-FITC (green), and

DAPI for nuclei (blue) as described in Materials and Methods. **(D)** Immunoblotting of mitochondrial lysates from T-Rex cells without doxycycline induction (lane 1), with doxycycline induction for 12 h (lane 2), and with doxycycline induction plus 25 μM H-7 (lane 3). Translocation of K-ras to the mitochondria was partially prevented by PKC inhibitor H-7. **(E)** K-ras activation (Tet/on) caused a decrease of mitochondrial transmembrane potential by 50% compared to control (off). Decrease of transmembrane potential was rescued by simultaneous treatment of H-7 (on + H-7). **(F)** K-ras-induced decrease of transmembrane potential was rescued by treatment with 5 μM cyclosporin A (on + CysA). **(G)** Quantitative analysis of transmembrane potential in K-ras-expressing cells in the presence or absence of cyclosporin A. Data are shown as mean ± SD. $n = 3$, $^{*}P < 0.05$, $^{**}P < 0.01$.

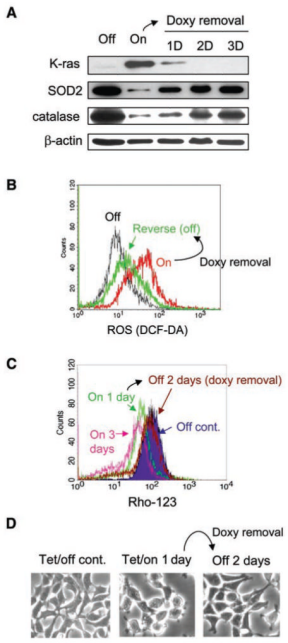

Figure 4.

Reversibility of K-ras^{G12V}-induced ROS generation and mitochondrial dysfunction. **(A)** T-Rex cells were treated with 20 ng/ml doxycycline for 24 h (Tet/on), followed by withdrawal of doxycycline from cell culture for 1, 2 and 3 days. Expression of K-ras, SOD2, catalase and β-actin was measured by western blot analysis. **(B)** K-ras induction (Tet/on) caused an increase of ROS. Removal of doxycycline for 2 days reversed ROS increase. **(C)** K-ras induction caused a decrease of mitochondrial transmembrane potential. Removal of doxycycline for 2 days reversed such decrease to baseline comparable to that of the control (Tet/off). **(D)** Morphology of HEK293 cells without K-ras^{G12V} expression (Tet/off), with K-ras^{G12V} expression for 1 day (Tet/on), and after withdrawal of doxycycline for 2 days.

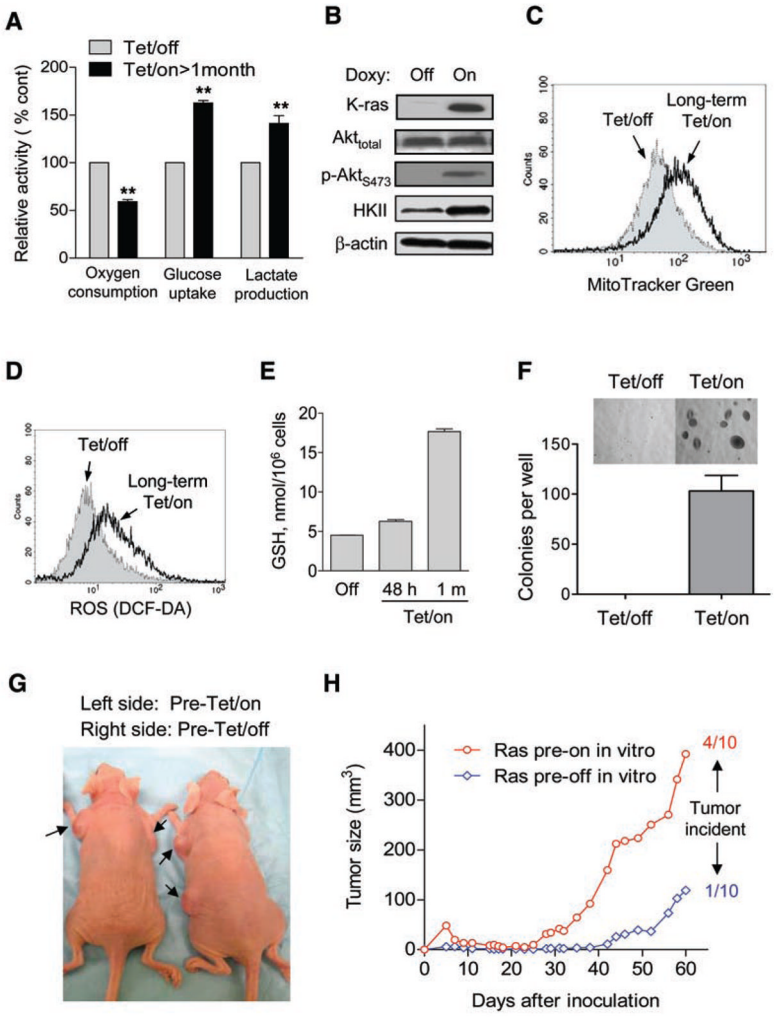

Figure 5.

Effect of long-term expression of K-ras^{G12V} on cellular metabolism and tumor formation capacity. **(A)** T-Rex/K-ras cells were induced to express K-RAS by continuous culture with 20 ng/ml doxycycline for over 1 month. Oxygen consumption, glucose uptake and lactate production were measured in comparison with the Tet/off control cells. **(B)** Western blot analysis of Akt and hexokinase II (HKII) in T-Rex/K-ras cells with or without long-term expression of K-ras. **(C)** Comparison of mitochondrial mass in Tet/off and long-term Tet/on cells, measured by flow cytometry analysis after staining with MitoTracker Green. **(D)** ROS production remained elevated after induction of K-ras^{G12V} for over a month (long-term Tet/on). **(E)** Analysis of glutathione (GSH) levels in T-Rex/K-ras cells without or with K-ras$_{G12V}$ induction for short term (48 h) and long term (> 1 month). **(F)** Comparison of T-Rex/K-ras cells with or without long-term pre-induction of K-ras^{G12V} for colony formation in soft agar. The same number of cells were seeded in soft agar suspension in a six-well plate described in Materials and Methods. After incubation for 15 days, colonies were stained with iodonitroterazolium violet and counted. Data are shown as mean ± SD from triplicate experiments. **(G)** Representative mice showing tumors grown from inoculated T-Rex/K-ras cells. Cells with and without long-term pre-induction of K-ras^{G12V} expression were inoculated into the left flank and right flank of the same mice, respectively. **(H)** Comparison of tumor growth in mice bearing T-Rex/K-ras cells with and without long-term

pre-induction of K-ras^{G12V} expression. After cell inoculation, all mice received doxycycline during the 60-day observation period.